The FitzHugh-Nagumo Model Dynamics with an Application to the Hypothalamic Pituitary Adrenal Axis

by

Rose Taj Faghih
B.S., Electrical Engineering (2008)
University of Maryland, College Park

Submitted to the Department of Electrical Engineering and Computer Science
in partial fulfillment of the requirements for the degree of

Master of Science in Electrical Engineering and Computer Science
at the
MASSACHUSETTS INSTITUTE OF TECHNOLOGY
June 2010

Author .....
Department of Electrical Engineering and Computer Science
May 7, 2010

Certified by .....
Munther A. Dahleh
Professor of Electrical Engineering and Computer Science
Thesis Supervisor

Certified by .....
Emery N. Brown
Professor of Computational Neuroscience and HST
Thesis Supervisor

Accepted by .....
Terry P. Orlando
Chair, Department Committee on Graduate Students

The FitzHugh-Nagumo Model Dynamics with an Application to the Hypothalamic Pituitary Adrenal Axis

by

Rose Taj Faghih

B.S., Electrical Engineering (2008)

University of Maryland, College Park

Submitted to the Department of Electrical Engineering and Computer Science
on May 7, 2010, in partial fulfillment of the
requirements for the degree of
Master of Science in Electrical Engineering and Computer Science

Abstract

In this thesis, I revisit the issue of the utility of the FitzHugh-Nagumo (FHN) model for capturing neuron firing behaviors. It has been noted (e.g., see [8]) that the FHN model cannot exhibit certain interesting firing behaviors such as bursting. I will illustrate that, by allowing time-varying parameters for the FHN model, one could overcome such limitations while still retaining the low order complexity of the FHN model. I also highlight the utility of the FHN model from an estimation perspective by presenting a novel parameter estimation method that exploits the multiple time scale feature of the FHN model, and compare the performance of this method with the Extended Kalman Filter through illustrative examples. Then, I apply this proposed extension to the FHN model to model cortisol secretion, which is controlled by the hypothalamic pituitary adrenal axis (HPA).

Existing mathematical models for cortisol secretion do not include the entire cortisol secretion process, from the neural firing of cortopin releasing hormone(CRH) in the hypothalamus to cortisol secretion in a deterministic manner. I lay the groundwork to construct a more comprehensive model, relating CRH, Adrenocorticotropic hormone (ACTH), and cortisol. I start with one of the existing cortisol mathematical models, and add to it a simplified neural firing model to describe the CRH and ACTH release. This simplified neural firing model is obtained using the FHN model with time-varying spiking threshold. Moreover, I include a feedback in this model and model the cortisol secretion as a tracking problem.

Thesis Supervisor: Munther A. Dahleh
Title: Professor of Electrical Engineering and Computer Science

Thesis Supervisor: Emery N. Brown
Title: Professor of Computational Neuroscience and HST

Acknowledgments

I would like to thank my advisors Professor Munther Dahleh and Professor Emery Brown for their guidance throughout the past two years; I consider myself a very fortunate graduate student for having the pleasure of being their student. I have learned a lot from them as a student in their classes and also as a member of their research groups. Their invaluable advice and ideas made this research possible. I am especially grateful to them for their unwavering support as well as their encouraging words when I needed them most.

I would like to thank Dr. Ketan Savla for devoting his valuable time mentoring me, listening to my thoughts and ideas, reading my drafts, and providing me with very insightful advice and ideas, without which I could not have obtained the results in this thesis. Also, I would like to thank Dr. Michael Rinehart for his valuable interactions with me for inverting the existing cortisol mathematical models. Moreover, I would like to thank my friends, officemates, and labmates for making my journey so far at MIT a wonderful experience.

I am also grateful to the National Science Foundation (NSF) for supporting my research through the NSF Graduate Research Fellowship. This research was also supported in part by an MIT Fellowship in Control.

I would like to thank Professor Thomas Antonsen, Professor Ed Ott, and Professor Michelle Girvan for introducing me to the field of computational neuroscience through studying the Kuramoto model as an undergraduate student. Especially, I would like to thank Professor Antonsen for being a great mentor and advisor, providing me with invaluable feedback when formulating my NSF research proposal.

Finally, I would like to thank my parents for believing in me, and their unconditional love and support. I would also like to thank my dearest brother Ali for being there for me all the time even if we were miles away from each other. It has been great to

have him here at MIT with me during this past year.

Contents

List of Figures

List of Tables

Chapter 1

Introduction

1.1 Dynamical Modeling of Neural Spiking

Hodgkin-Huxley (HH) could be considered as the most successful dynamical model in computational neuroscience for capturing neural firing behaviors. Although this model is capable of generating all the behaviors of neuron spiking, it is a highly nonlinear model with many coefficients. In this thesis, I will show that most of the neural firing activities of interest that are possible by well-known dynamical systems models (such as the HH model) could be obtained using *low complexity* dynamical models. In the first part of this thesis, I will propose an extension to the FitzHugh-Nagumo model that includes a time-varying spiking threshold, which is physiologically programmed within the neuron. Then, I will discuss some of the interesting neural spiking activities that this *low complexity* dynamical model can generate.

1.2 Parameter Estimation of a Low Complexity Neural Spiking Dynamical Model

Considering the low complexity of the FHN model and the proposed extension to it, one could investigate the slow and fast dynamics of the FHN model to estimate its parameters. In the second part of this thesis, I will propose an algorithm for estimating the spiking threshold of the FHN model and compare the performance of this method with the Extended Kalman Filter (EKF) for fixed spiking threshold. Then, I will extend this algorithm to the case that the FHN model has a time-varying firing threshold, and again compare the performance of this algorithm to EKF.

1.3 An Application to Feedback Control Modeling of Cortisol Secretion

Existing mathematical models for cortisol secretion do not include the entire cortisol secretion process, from the neural spiking in the hypothalamus to cortisol secretion in a deterministic manner. The proposed extension to the FHN model could be used to model the spiking activity that results in cortisol secretion. In the last part of this thesis, I start with one of the existing cortisol mathematical models, and add to it a neural firing model. Then, I extend the existing model by including the negative feedback effect of cortisol level on cortisol secretion, and propose a more comprehensive model.

Chapter 2

FitzHugh-Nagumo Model with Time-varying Spiking Threshold

2.1 Dynamical Models in Computational Neuroscience

Since the seminal work of Hodgkin and Huxley, there has been a continued interest in the dynamical systems viewpoint of a neuron. Hodgkin-Huxley (HH), Hindmarsh-Rose (HR), and FitzHugh-Nagumo (FHN) models are among the most successful dynamical models in computational neuroscience for capturing neural firing behaviors. A detailed explanation of these and several other models can be found in [8]. The HH model consists of four differential equations with a high number of coefficients. Although this model is capable of generating all the behaviors of neuron spiking, it is a highly nonlinear model. The HR model, on the other hand, consists of three differential equations, which are highly coupled, and it can exhibit all the firing modes obtained from the HH model except for biophysically meaningful behaviors [7]. Finally, the FHN model consists of two differential equations, and is simpler than the HH and HR models, though it is unable to exhibit important firing behaviors such

as bursting. In fact, it has been noted [7] that without using a reset or adding noise, the FHN model can not exhibit bursting. The focus of this thesis is on *low complexity* dynamical models that can exhibit most of the neural firing activities of interest that are possible by well-known dynamical systems models (such as the HH model) but are nevertheless of low complexity. Here, we use the term complexity to refer to the presence of redundancies in the model on top of its capability to capture neural firing behaviors, difficulty in parameter estimation and from the control viewpoint. With this in mind, we propose an extension of the FHN model with time-varying parameters, where the hypothesis is that the time variations of these parameters are either physiologically programmed within a neuron or are coupled to the output of the typical hormone generating systems that are triggered by the neural firings, e.g. the negative feedback effect of cortisol level on the neurons in the hypothalamus [3].

2.2 The FitzHugh-Nagumo Model

As mentioned above, a simplified version of the HH model is the FHN model:

$$\frac{dv}{dt} = a(-v(v-1)(v-b) - w + I)$$

$$\frac{dw}{dt} = v - cw$$

where v is the membrane potential, w is the recovery variable, a and c are scaling parameters, and I is the stimulus current. Moreover, b is an unstable equilibrium that corresponds to the threshold between electrical silence and electrical firing [1]. It is recommended to choose $a >> 1$ [14], $0 < c$ and small enough [18]. Also, b should be between zero and one, and to obtain suitable supra-threshold behavior, usually $b < 0.5$ is chosen [24]. For appropriate constant parameters, it is possible to generate tonic firing using FHN, where tonic firing is referred to as a firing behavior in which the neuron spikes in a periodic manner.

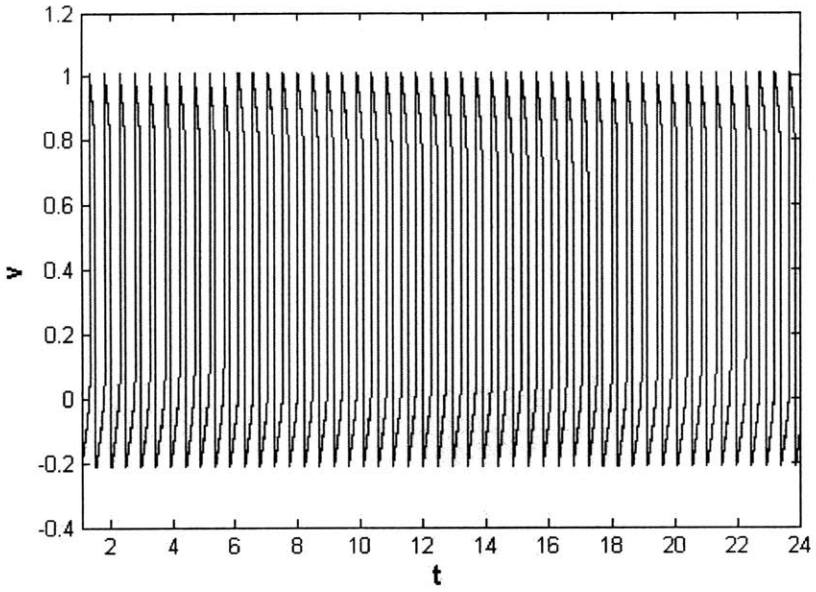

Figure 2-1: Tonic Firing

Considering that conventionally the parameters in the FHN model are kept constant, certain firing behaviors such as bursting can not be obtained using this model[8]. Since I is an external input, it can externally control the firing mode observed in the output (v), and result in firing behaviors such as bursting [23]; on the other hand, the parameters a, b, and c are governed by the mechanisms internal to the neuron, and their variations can be associated to some internal physiological system. Hence, it is more interesting to vary those parameters to generate behaviors such as bursting because this method adds a totally internal firing capability to the system. In this project, we consider variations in b because b is the threshold between electrical silence and neural firing, and physiologically, it might be the case that this threshold is varying throughout the day, causing the neurons to switch on and off, and generate bursting. Since b can control both the firing frequency and amplitude, we propose that by varying b in FHN, it is possible to obtain firing modes such as bursting.

2.3 The FitzHugh-Nagumo Model with Time-Varying Threshold

Since b can control both the firing frequency and amplitude, we propose that by varying b in FHN, it is possible to obtain firing modes such as bursting. Hence, we will vary b using different functions, and discuss the observed behaviors through illustrative examples. In other words, our proposed model adds to FHN another differential equation $\frac{db}{dt} = g(t)$, where g(t) is a function of time that is determined based on the physiology of the neuron.

The following is our proposed extension to FHN model, which includes the time-varying threshold:

$$\frac{dv}{dt} = a(-v(v-1)(v-b) - w + I)$$

$$\frac{dw}{dt} = v - cw$$

$$\frac{db}{dt} = g(t)$$

In the following subsections, we will show that using this approach, spiking patterns such as tonic bursting, mixed mode firing, neural firing with non-increasing frequency, and varying frequency neural firing can be obtained. The simulations were performed in Simulink.

2.3.1 Tonic Bursting

Tonic bursting is a firing behavior in which a neuron fires a certain number of spikes and is silent for a certain amount of time. Then, it repeats this pattern in a periodic manner. To simulate tonic bursting using FHN, we keep a, I, and c at constant values 10^5, 1, and 0.2, respectively, and vary b using two different method as follows:

1. First, b was varied using a sinusoidal function $b(t) = 0.5 + 0.5sin(\frac{\pi}{6}t)$ and tonic bursting was obtained as observed in Fig. 2-2.

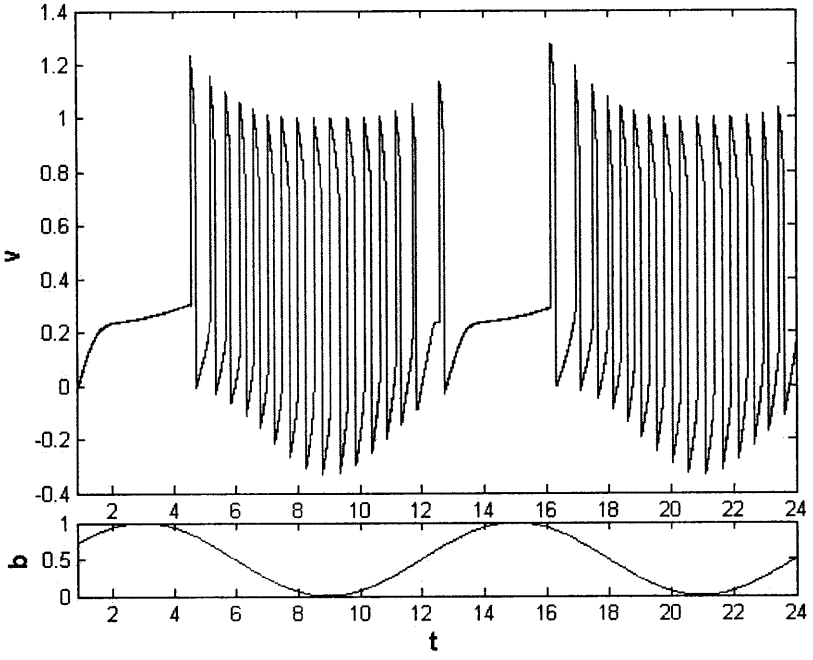

Figure 2-2: Tonic Bursting using a sinusoidal b

2. Then, b was varied using:

$$b(t) = \begin{cases} \frac{(t-6)^2}{36} & t < 12 \\ \frac{(t-18)^2}{36} & 12 \leq t < 24 \end{cases}$$

where this function could be repeated periodically with a period of 24. Tonic bursting was obtained as observed in Fig. 2-3.

These are two possible ways of varying b in order to obtain tonic bursting. Different sinusoidal functions, triangular waves, or combinations of polynomials could also be used for obtaining tonic bursting.

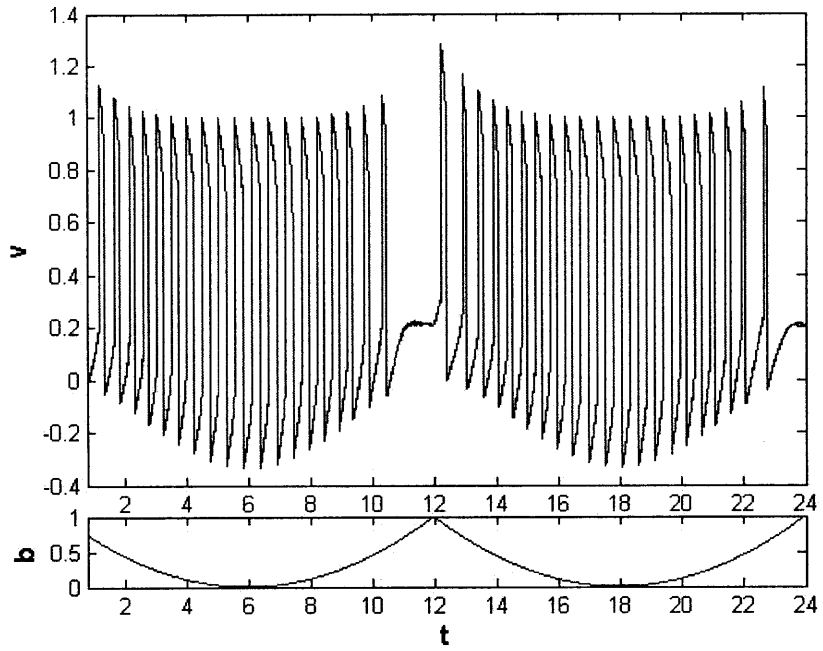

Figure 2-3: Tonic Bursting using a polynomial b

2.3.2 Mixed Mode Firing

Mixed mode is a firing mode in which the neuron fires a single burst when the stimulus is applied and then switches to tonic spiking [7]. To simulate mixed mode firing using FHN, we keep a, I, and c at constant values 10^5, 1, and 0.2, respectively, and vary b in the beginning using a sinusoidal function followed by keeping it at a constant value as follows:

$$b(t) = \begin{cases} 0.5 + 0.5sin(\frac{\pi}{2}t) & t < 6.5 \\ 0.1464 & 6.5 \leq t < 24 \end{cases}$$

where this function could be repeated periodically with a period of 24. As observed in Fig. 2-4 a mixed mode firing pattern was obtained using this method. This is one possible way of generating mixed mode. Another way could be to use a triangular wave or a sinusoidal function at the beginning, and then keep the value of b constant.

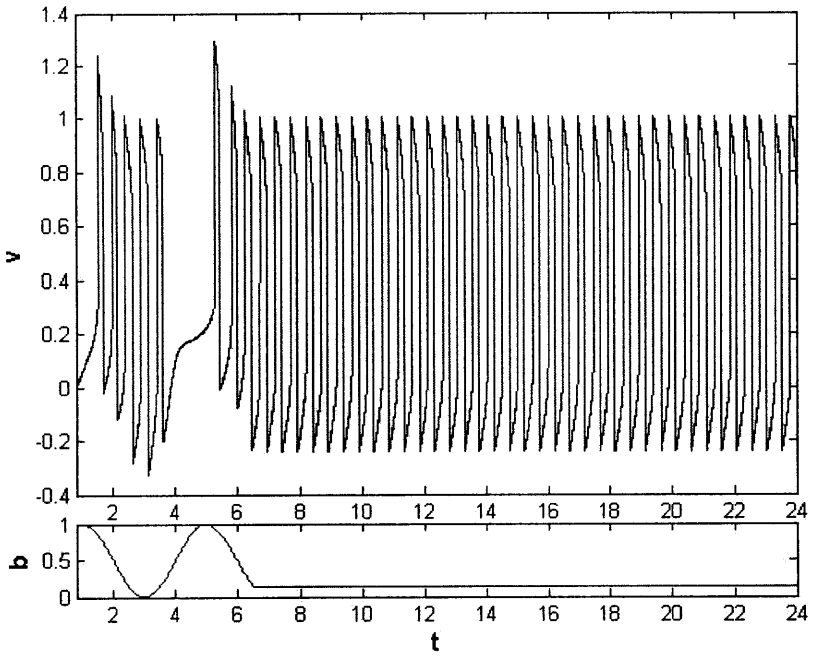

Figure 2-4: Mixed Mode Firing

2.3.3 Neural Firing with Non-increasing Frequency

Neural firing with non-increasing frequency is another possible firing mode obtained by varying b. To simulate a neural firing mode with non-increasing frequency, we keep the parameters a, I, and c fixed at constant values 10^5, 1, and 0.25, respectively, and first start with slowly increasing b using a linear function, and then keep b at a constant value. For the simulation in Fig. 2-5, b was varied as follows:

$$b(t) = \begin{cases} \frac{1}{24}t & t < 12 \\ 0.5 & 12 \leq t < 24 \end{cases}$$

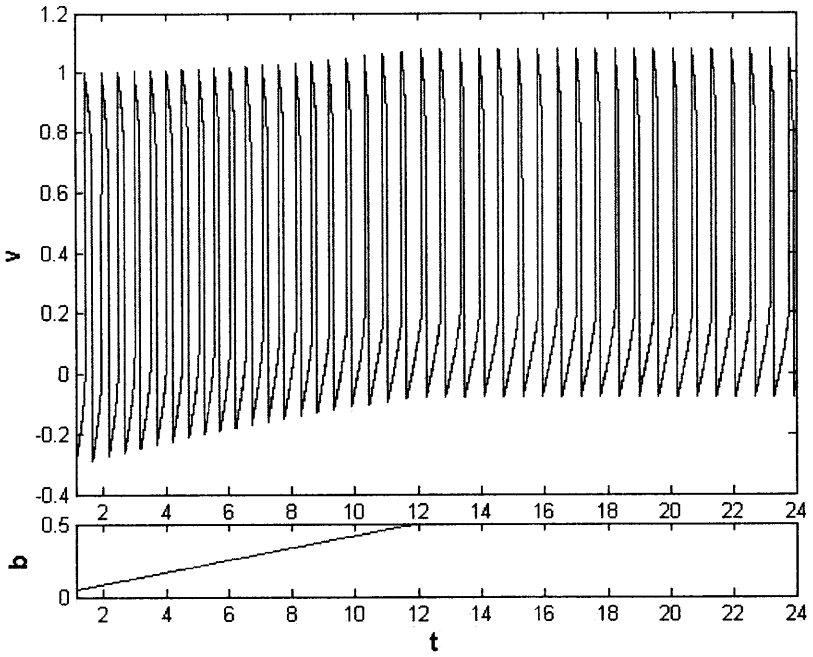

Figure 2-5: Neural Firing with Non-increasing Frequency

2.3.4 Varying Frequency Neural Firing

Finally, we will illustrate that neural firing with varying frequency can be obtained using FHN. To simulate this firing mode, we keep the parameters a, I, and c fixed at constant values 10^5, 1, and 0.3, respectively, while varying b using two different methods as follows:

1. First, b was varied using a two-harmonic function as observed in Fig. 2-6. For this simulation, we defined b as:
   $b(t)=\frac{10-6cos(\frac{2\pi}{24}t)+3.5sin(\frac{2\pi}{24}t)-3.5cos(\frac{4\pi}{24}t)-1.1720sin(\frac{4\pi}{24}t)}{30}$.
   However, it is possible to use other two-harmonic functions to obtain the desired behavior.

2. Then, b was varied a follow: $b(t) = (t-12)^2/144, t < 24$, and a firing mode with varying frequency was obtained as observed in Fig. 2-7. This function can

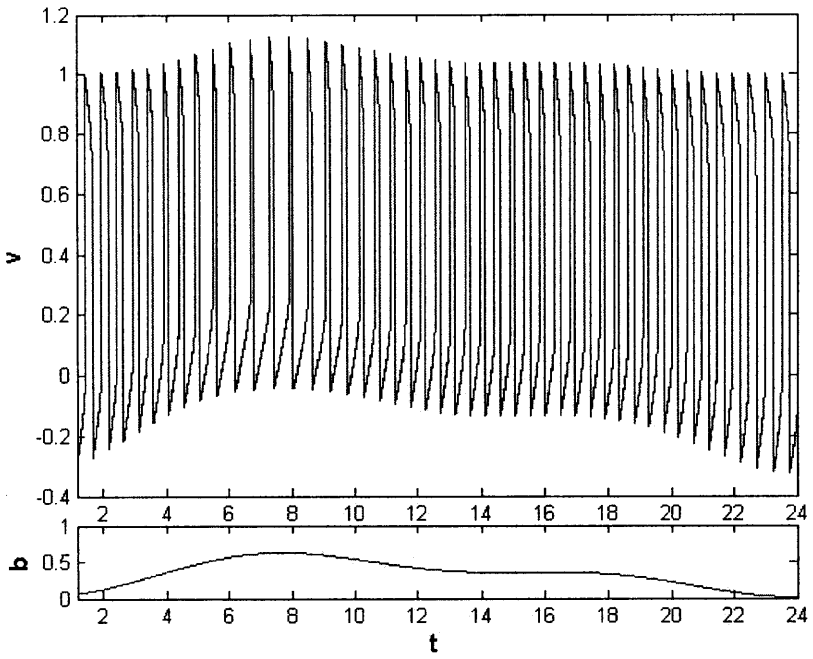

Figure 2-6: Varying Frequency Neural Firing using a two-harmonic b

be repeated periodically with a period of 24.

These are two possible ways of varying b in order to obtain varying frequency neural firing. Other combinations of sinusoidal or polynomial functions could also be used for obtaining such behavior.

These examples suggest that by varying the parameters that are internal to FHN, one could obtain richer set of behaviors.

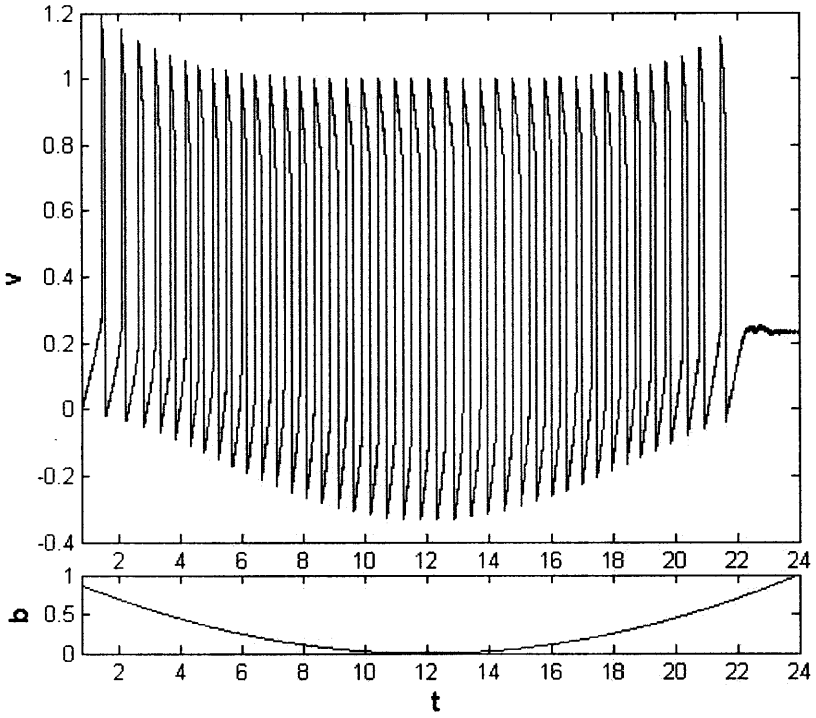

Figure 2-7: Varying Frequency Neural Firing using a polynomial b

Chapter 3

Estimation Algorithm for Constant Spiking Threshold in FitzHugh-Nagumo Model

3.1 Parameter Estimation in Computational Neuroscience

In computational neuroscience, parameter estimation for dynamical models such as Hodgkin-Huxley (HH), Hindmarsh-Rose (HR), and FHN is usually done using *standard* methods such as Simulated Annealing, Genetic Algorithms, Differential Evolution [4], Adaptive Observer, or Extended Kalman Filter (EKF) [22]. However, in principle, if the model has relevant structure, one could exploit it to formulate a parameter estimation method customized to that model and tune it to get better performance than the standard methods. By investigating the slow and fast dynamics of the FitzHugh-Nagumo model, one could estimate the parameters of FHN. In this chapter, we will employ the dynamics of the FHN model to propose a novel estimation algorithm for estimating the threshold between electrical firing and electrical silence.

Then, we will compare the performance of this method with the Extended Kalman Filter (EKF) for the fixed parameter case through illustrative examples. The examples demonstrate that this estimation method outperforms EKF when the sensor covariance is large or when the sampling rate is low.

3.2 Estimating b Using Fast-Slow Dynamics of the FitzHugh-Nagumo Model

The phase portrait shows that, in case of tonic firing mode, the trajectories switch between *slow scale dynamics* and *fast scale dynamics*. Considering the dynamics of the FHN model, we propose to develop a novel estimation algorithm that exploits the multiple time-scale feature of FHN. To do so, we will start with a time-series plot of action potentials v that are firing in a tonic manner, and develop an algorithm to estimate b. We will only look at the time scale features of one firing that occurs on the limit cycle. Fig. 3-1 is a representation of the slow and fast dynamics of FHN on the wv-plane and its corresponding behavior with respect to the time-series plot of v.

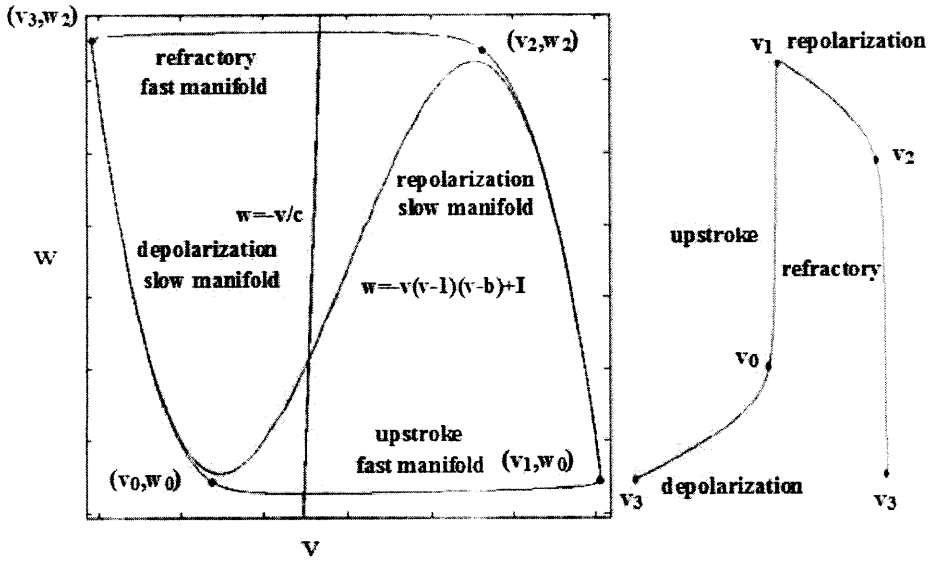

Figure 3-1: Phase Portrait (left) and Time-series Plot (right): a=1369, b=0.2, I=1, c=0.3

Since v does not change much when the system is following the slow time scale dynamics of FHN, we will approximate its derivative as zero. $\frac{dv}{dt} = 0 \Rightarrow w = -v(v-1)(v-b) + I$. Then, define f as:

$$f(v, b, I) = -v(v-1)(v-b) + I$$

Let v_2 and v_0 be the values of v that maximize and minimize f:

$$v_0 = \frac{1}{3}(b + 1 - \sqrt{b^2 - b + 1}),$$
$$v_2 = \frac{1}{3}(b + 1 + \sqrt{b^2 - b + 1})$$

As observed in Fig. 3-1, w_2 and w_0 do not exactly correspond to maximum and minimum values of f; however, we can approximate w_2 and w_0 by plugging in the values of v_2 and v_0 in $f(v, b, I)$, as shown below:

$$w_0 \approx \frac{2}{27}b^3 - \frac{1}{9}b^2 - \frac{2}{27}b^2\sqrt{b^2 - b + 1} - \frac{1}{9}b$$
$$+\frac{2}{27}b\sqrt{b^2 - b + 1} + \frac{2}{27} - \frac{2}{27}\sqrt{b^2 - b + 1} + I$$
$$w_2 \approx \frac{2}{27}b^3 - \frac{1}{9}b^2 + \frac{2}{27}b^2\sqrt{b^2 - b + 1} - \frac{1}{9}b$$
$$-\frac{2}{27}b\sqrt{b^2 - b + 1} + \frac{2}{27} + \frac{2}{27}\sqrt{b^2 - b + 1} + I$$

Let $h_0(b) = w_0 - I$ and $h_2(b) = w_2 - I$. Then,

$$h_0(b) - h_2(b) = -\frac{4}{27}\sqrt{(b^2 - b + 1)^3} \approx -0.21b^2 + 0.21b - 0.15$$

From the time series data of membrane potentials, it is possible to obtain the maximum and minimum values of v, v_1 and v_3, respectively. As observed in Figure 3-1:

$$f(v_1, b, I) \approx w_0 \Rightarrow -v_1(v_1 - 1)(v_1 - b) + I \approx w_0 \approx h_0(b) + I$$

$$f(v_3, b, I) \approx w_2 \Rightarrow -v_3(v_3 - 1)(v_3 - b) + I \approx w_2 \approx h_2(b) + I$$

Hence, we obtain:

$$-v_1(v_1 - 1)(v_1 - b) \approx h_0(b)$$
$$-v_3(v_3 - 1)(v_3 - b) \approx h_2(b)$$

Since there are two equations and one unknown, the system might not have a solution; in cases that the system has a solution, the solution can be obtained using equation (3.1):

$$\begin{aligned} &-v_1(v_1 - 1)(v_1 - b) + v_3(v_3 - 1)(v_3 - b) \\ &= h_0(b) - h_2(b) = -\frac{4}{27}\sqrt{(b^2 - b + 1)^3} \end{aligned} \tag{3.1}$$

For simplicity in the computation, we use the following approximation to equation 3.1:

$$\begin{aligned} &-v_1(v_1 - 1)(v_1 - b) + v_3(v_3 - 1)(v_3 - b) \\ &= h_0(b) - h_2(b) \approx -0.21b^2 + 0.21b - 0.15 \end{aligned}$$

Let $h_b = -v_1(v_1 - 1)(v_1 - b) + v_3(v_3 - 1)(v_3 - b) + 0.21b^2 - 0.21b + 0.15$. Setting $h_b = 0$, two values for b are obtained, and considering that b takes on a value between zero and one, the value of b that satisfies this bound is the desired solution. In the cases that both solutions satisfy the bound, we plug both values of b into equation (3.1), and the value that minimizes the absolute value of the difference between the two sides of equation (3.1) is the desired value of b. If a b value is not obtained using this approach, we will find the value of b that minimizes h_b. If this value still does not satisfy the bound, one could plug in values zero and one into equation (3.1), and the value that minimizes the absolute value of the difference between the two sides of equation (3.1) is the desired value of b.

Using parameters a=10^5, I=1, c=0.3 for the FHN model, and starting with b=0.05 and increasing the b value in 0.05 increments until the system does not have a tonic behavior (b=0.75), we obtained different time-series plots of membrane potentials. Then, for each of these time-series plots, we estimated b using the method described

above; the estimated values as well as the percent errors are shown in Table 3.1. As observed in Table 3.1, the error varies between 0.42% and 5.20%.

Table 3.1: Estimates of b using the FSD method

b	$b_{estimate}$	percent error
0.05	0.0526	5.2000
0.1	0.1034	3.4000
0.15	0.1540	2.6667
0.2	0.2044	2.2000
0.25	0.2546	1.8400
0.3	0.3048	1.6000
0.35	0.3552	1.4857
0.4	0.4064	1.6000
0.45	0.4612	2.4889
0.5	0.5021	0.4200
0.55	0.5378	2.2182
0.6	0.5929	1.1833
0.65	0.6441	0.9077
0.7	0.6944	0.8000

3.3 Comparison with Extended Kalman Filter

In the previous section, a novel approach for estimating b was proposed. In this section, we compare the b estimates given by the Fast-Slow Dynamics (FSD) estimation algorithm and EKF. In order to compare our estimation method with EKF, process noise and sensor noise were incorporated into the simulations using the following model:

$$\frac{dv}{dt} = a(-v(v-1)(v-b) - w + I) + N(0, \sigma_p^2)$$

$$\frac{dw}{dt} = v - cw + N(0, \sigma_p^2)$$

$$\frac{db}{dt} = N(0, \sigma_p^2)$$

$$v_{obs} = v + N(0, \sigma_s^2)$$

where σ_p and σ_s represent the standard deviation in the process noise and the sensor noise, respectively. Moreover, v_{obs} is the observed membrane potential. In order to implement EKF, we discretized the system using Euler forward method with a sampling rate Δ. For this comparison, v was simulated using a=10^5, I=1, c=0.3, b = 0.5 while adding a zero-mean normal process noise with a standard deviation of 0.1 (σ_p=0.1), and the sampling rate and sensor noise were varied as discussed in the following three examples. Moreover, we averaged the data for 24 tonic firings to run FSD and implemented EKF while using the actual initial condition values as the initial guess, and an initial covariance estimate of zero.

1. A zero-mean sensor noise with σ_s=0.001 was added to the simulated membrane potentials for Δ=10^{-5}. Using our method, a b estimate of 0.5079 (1.58% error) was obtained. Then, EKF was implemented on the data, and the estimated value of b after one limit cycle was 0.5001 (0.02% error). In this simulation, the sampling rate was very high and the sensor noise was very low, putting EKF in an advantage. However, by increasing the sensor noise or decreasing the sampling rate, our method performed better than EKF.

2. By adding zero-mean sensor noise with σ_s=0.01 to the simulated action potentials, and using Δ=10^{-5}, a b estimate of 0.5253 (5.06% error) was obtained using our method while b estimates for EKF did not converge and varied between 0.1358 and 1.47.

3. For Δ=10^{-3}, and a zero-mean sensor noise with σ_s=0.001, we implemented both FSD and EKF. Using FSD a b estimate of 0.5175 (3.5% error) was obtained, while EKF diverged.

Hence, comparing the two methods, EKF is more sensitive to sampling rate than our method. This could be because our method only requires the knowledge of the maximum and minimum voltage values, and when we decrease the sampling rate, the maximum and minimum values obtained are close to the actual ones. Moreover, EKF

does not converge if the sensor noise covariance is large.

In the next chapter, we will extend this algorithm to the case when this threshold is varying and one has more knowledge about the structure of the variations (e.g., oscillatory, impulsive, etc.) of this parameter. To do so, we will use some standard statistical methods such as multiple regression in addition to our estimation method.

Chapter 4

Estimation Algorithm for Time-varying Spiking Threshold in FitzHugh-Nagumo Model

In the previous chapter, an algorithm for estimating b was proposed. In this chapter, using examples, we will illustrate that the Fast-Slow Dynamics (FSD) estimation algorithm for constant b can be employed on the neural firing data that is generated by time-varying b. To implement the algorithm on the data, first one should obtain multiple datasets, and use the average of these datasets in order to estimate the parameters to reduce the effect of noise. In order to run FSD for time-varying b, one could find the membrane potential peaks, and break the data into smaller data sets, in a way that each smaller dataset starts at one peak and ends at the following peak (in other words, one could break the data points in a way that each of these smaller datasets goes through the limit cycle once). Then, using our algorithm for estimating constant b, one could estimate b for each of these smaller datasets, and associate each of these estimates with the time that the second peak is observed. Then, if one has prior knowledge about the structure of b, one could implement multiple or linear regression (depending on the structure of b) to fit a function to the b estimates

obtained using FSD method. In the cases that b follows two (or more) different functions as a function of time, one could break the data into two (or more) parts at the the point(s) that the variations in the function occur, and depending on the kind of function b is following, linear or multiple regression could be used to fit the b estimates for each part of the data. In the following two sections, we will implement FSD method on neural firing with non-increasing frequency and varying frequency neural firing. Then, we will implement our estimation method on tonic bursting, and compare its performance with EKF.

4.1 Parameter Estimation for Neural Firing with Non-increasing Frequency

Neural firing with non-increasing frequency was obtained by incorporating process noise and sensor noise into the simulations using the following model:

$$\frac{dv}{dt} = a(-v(v-1)(v-b) - w + I) + N(0, \sigma_p^2)$$

$$\frac{dw}{dt} = v - cw + N(0, \sigma_p^2)$$

$$\frac{db}{dt} = \begin{cases} \alpha + N(0, \sigma_p^2) & t < 12 \\ N(0, \sigma_p^2) & 12 \leq t < 24 \end{cases}$$

$$v_{obs} = v + N(0, \sigma_s^2)$$

where σ_p and σ_s represent the standard deviation in the process noise and the sensor noise, respectively. Moreover, v_{obs} is the observed membrane potential. b first starts increasing as a linear function with slope α, and then remains constant. In other

words, b is of the form:

$$b(t) = \begin{cases} \alpha t + \beta & t < t_0 \\ \alpha t_0 + \beta & t_0 \leq t < 24 \end{cases}$$

We simulated 5 datasets using this system of equations by letting a=10^5, I=1, c=0.25, σ_p=10^{-2}, and σ_s=10^{-3}, and averaged the five datasets. Then, we broke the dataset into smaller parts and implemented FSD algorithm to obtain a vector of b estimates. Then, by plotting these b estimates as a function of time, and inspecting the b estimates, we obtained the b value at which b remains constant. Then, we broke the b estimates into two sets. One set included the b estimates that were following the linear function, and the other set included the approximately constant b estimates. We estimated α and β by implementing linear regression on the first dataset, and obtained an estimate for the constant b by taking the mean of the second dataset. Then, t_0 was obtained by letting the constant b estimate equal to $\alpha t_0 + \beta$ and solving for t_0. Fig. 4-1 is a plot of b and its estimate.

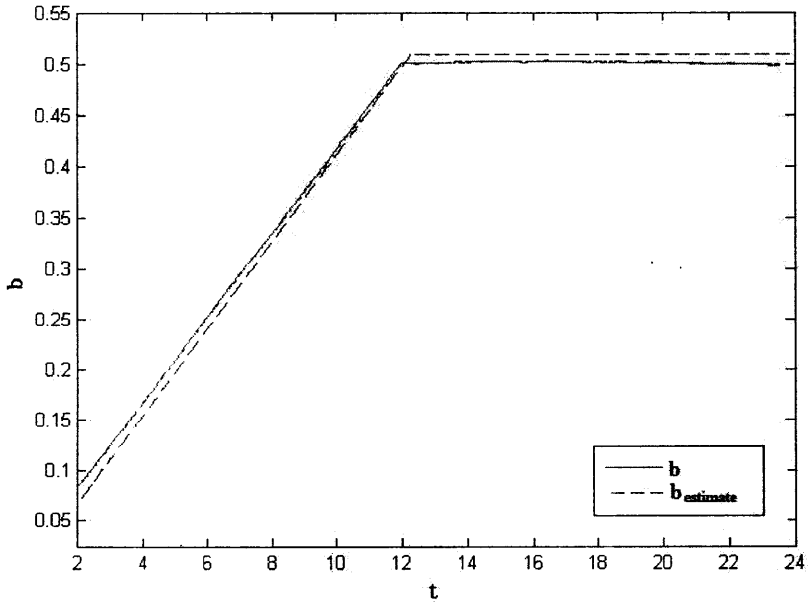

Figure 4-1: Parameter Estimation for Neural Firing with Non-increasing Frequency Using FSD Algorithm

4.2 Parameter Estimation for Varying Frequency Neural Firing

Neural firing with non-increasing frequency was obtained by incorporating process noise and sensor noise into the simulations using the following model:

$$\frac{dv}{dt} = a(-v(v-1)(v-b) - w + I) + N(0, \sigma_p^2)$$

$$\frac{dw}{dt} = v - cw + N(0, \sigma_p^2)$$

$$\frac{db}{dt} = -\frac{2\pi}{24}\beta sin(\frac{2\pi}{24}t) + \frac{2\pi}{24}\gamma cos(\frac{2\pi}{24}t) - \frac{2\pi}{12}\zeta sin(\frac{2\pi}{12}t) + \frac{2\pi}{12}\kappa cos(\frac{2\pi}{12}t) + N(0, \sigma_p^2)$$

$$v_{obs} = v + N(0, \sigma_s^2)$$

where σ_p and σ_s represent the standard deviation in the process noise and the sensor noise, respectively. Moreover, v_{obs} is the observed membrane potential. b is a two-harmonic function with periods 24 and 12 (e.g. b could be governed by the circadian rhythm). In other words, b is of the form:

$b(t)=\alpha + \beta cos(\frac{2\pi t}{24}) + \gamma sin(\frac{2\pi t}{24}) + \zeta cos(\frac{2\pi t}{12}) + \kappa sin(\frac{2\pi t}{12})$

We simulated 5 datasets using the above system of equations by letting a=10^5, I=1, c=0.3, σ_p=10^{-2}, and σ_s=10^{-3}, and averaged the five datasets. Then, we broke the dataset into smaller parts and implemented FSD algorithm to obtain a vector of b estimates. Then, knowing that b was a two-harmonic function, we estimated α, β, γ, ζ, and κ by implementing multiple regression. Fig. 4-2 is a plot of b and its estimates.

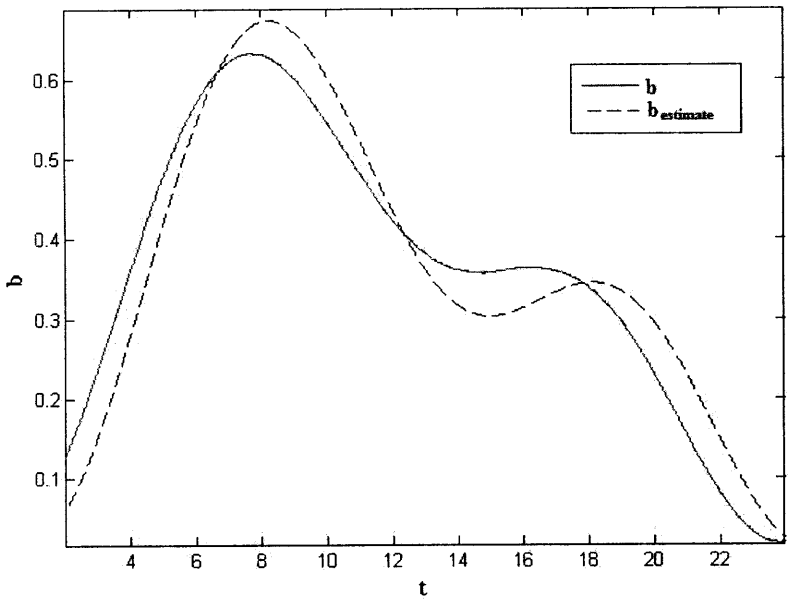

Figure 4-2: Parameter Estimation for Varying Frequency Neural Firing Using FSD Algorithm

4.3 Comparison of FSD and EKF Performance for Tonic Bursting

We will compare FSD estimation algorithm with EKF for tonic bursting, which can be obtained using a sinusoidal b. For this comparison, process noise and sensor noise were incorporated into the simulations using the following model:

$$\frac{dv}{dt} = a(-v(v-1)(v-(\alpha sin(\lambda t+\beta)+\gamma)) - w + I) + N(0,\sigma_p^2)$$

$$\frac{dw}{dt} = v - cw + N(0,\sigma_p^2)$$

$$\frac{d\gamma}{dt} = N(0,\sigma_p^2)$$

$$\frac{d\alpha}{dt} = N(0,\sigma_p^2)$$

$$\frac{d\lambda}{dt} = N(0,\sigma_p^2)$$

$$\frac{d\beta}{dt} = N(0, \sigma_p^2)$$

$$v_{obs} = v + N(0, \sigma_s^2)$$

σ_p and σ_s represent the standard deviation in the process noise and the sensor noise, respectively. Moreover, v_{obs} is the observed membrane potential. In order to implement EKF, we discretized the system using Euler forward method with a sampling rate Δ. For this comparison, v was simulated using a=10^5, I=1, c=0.3, $b = 0.5$ while adding a zero-mean normal process noise with σ_p=0.1, and the sampling rate and sensor noise were varied as discussed in the following three examples. We simulated five datasets using this method for each of the following examples, and used the average of these datasets in order to estimate the parameters. In order to run FSD for time-varying b, we found the membrane potential peaks, and broke the data into smaller data sets, in a way that each smaller dataset started at one peak and ended at the following peak (in other words, we break the data points in a way that each of theses smaller datasets goes through the limit cycle once). Then, using our algorithm for estimating constant b, we estimated b for each of these smaller datasets. Then, we associated each of these estimates with the time that the second peak was observed. Let $\lambda = \frac{2\pi}{T}$. Knowing that b was a sinusoid of the form $\alpha sin(\frac{2\pi}{T}t+\beta)+\gamma$, we found the period by looking at the time series plot of the b estimates, and then using the trigonometric identity, we rewrote this problem as $\alpha sin(\frac{2\pi}{T}t)cos(\beta) + \alpha cos(\frac{2\pi}{T}t)sin(\beta) + \gamma$, and implemented multiple regression to find the coefficients α, β, and γ. In order to implement EKF, we used the actual initial condition values as the initial guess, and an initial covariance estimate of zero.

1. After adding a zero-mean sensor noise with σ_s=0.001 to data with Δ=10^{-5}, we implemented FSD and EKF. The parameter estimates and the corresponding percent error for each of the parameters is reported in Table 4.1. In reporting the EKF estimate, we ignored the estimates for which the error covariance matrix becomes very high.

2. By adding a zero-mean sensor noise with σ_s^2=0.1, and using Δ=10^{-5}, we im-

Table 4.1: Comparison of parameter estimation obtained by FSD and EKF for example 1 for time-varying b

	FSD estimate	FSD error	EKF's estimate	EKF's error
α=0.5	0.4926	1.48%	0.5	0%
T=12	11.933	0.5583%	12	0%
cos(β)=1	0.9804	1.9558%	1	0%
γ=0.5	0.4937	1.26%	0.5	0%

plemented FSD and EKF. The EKF parameter estimates became very noisy; however, the average value of the noisy parameter estimates obtained by EKF had a small error, and here we are reporting the average value of the noisy estimates as the EKF parameter estimate. The parameter estimates and the corresponding percent error for each of the parameters is reported in Table 4.2

Table 4.2: Comparison of parameter estimation obtained by FSD and EKF for example 2 for time-varying b

	FSD estimate	FSD error	EKF's estimate	EKF's error
α=0.5	0.5708	4.72%	0.5045	0.9%
T=12	11.933	0.5583%	12.1461	1.2176%
cos(β)=1	0.9944	0.56%	1	0%
γ=0.5	0.5602	12.04%	0.5062	1.24%

3. For $\Delta=10^{-3}$, and a zero-mean sensor noise with σ_s=0.001, using our method parameter estimates reported in Table 4.3 were obtained, while EKF diverged.

Table 4.3: Comparison of parameter estimation obtained by FSD and EKF for example 3 for time-varying b

	FSD estimate	FSD error	EKF's estimate	EKF's error
α=0.5	0.4638	7.24%	Diverged	NA
T=12	12.029	0.2417%	Diverged	NA
cos(β)=1	0.9215	7.8511%	Diverged	NA
γ=0.5	0.4996	0.08%	Diverged	NA

In this chapter, through three examples, we showed how one could implement the FSD method for the case that b is a time-varying function. Then, comparing this algorithm

with EKF, we showed that this parameter estimation method performed better than EKF when the sampling rate was low. Another advantage of this estimation method over EKF is that for cases that the structure of b is unknown e.g. the underlying structure of b that governs the release of the cortopin releasing hormone, discrete b estimates can be obtained using our method to add insight to the underlying structure. On the other hand, EKF can not estimate the coefficients if the underlying structure of b is not known.

A physiological application of the FHN model with time-varying b could be the neural spiking that results in cortisol secretion. In the next chapter, we will discuss the mathematical models for cortisol. Then, we will propose a model for cortisol secretion that utilizes FHN model with time-varying b.

Chapter 5

Mathematical Modeling of Diurnal Cortisol Patterns

5.1 Hormones

Hormones could be considered as chemical messengers, relaying signals from one group of cells to another; hormone secretion is governed by circadian rhythm, which is a biological clock with a period of 24 hours [5]. Hormone secretion can be stimulated by neurons in the hypothalamus. In neurons, oscillatory changes in the membrane potentials as well as the intracellular Ca^{2+} oscillations result in neurosecretion in a pulsatile manner [21]. Neurosecretion is the coupling of electrical activity to hormone release, and the amount of hormone released by spiking increases as the frequency of spikes increases [17]. In other words, the periodic increase in hormone release is a consequence of synchronization in hormone generating neurons as well as increase in firing activity in individual neurons instead of using new neurons [21]. Pulsatile neurosecretion results from synchronized bursting activity of neuroendocrine cells[17], and intracellular chemical concentrations play an important role in releasing hormones. For example, in Luteinizing Hormone-Releasing Hormone (LHRH) neurons,

high K^+ results in neurosecretion, which is followed by an increase in Ca^{2+} , and oscillatory changes in membrane potentials. Moreover, Nitric Oxide (NO) meditates the release of the LHRH [21]. This chapter provides an introduction to cortisol, a steroid hormone, and cortisol secretion, from neural firing to cortisol concentration in the plasma and discusses a selection of the mathematical models of cortisol patterns.

5.2 Cortisol Secretion

Cortisol is a steroid hormone that regulates the metabolism and body's reaction to stress and inflammation [3]. Stress can be physical, such as infection, thermal exposure, and dehydration, or psychological, such as fear and anticipation [9]. Cortisol relays rhythmic signals from the suprachiasmatic nucleus (SCN), the circadian pacemaker, to synchronize bodily systems with environmental variations [19]. Cortisol secretion can be stimulated by calcium oscillations and changes in the membrane potential of the hypothalamus neurons. Moreover, ultradian analysis of cortisol shows significant periods of 24 hours, 12 hours, and 2 hours. The first two significant periods (24 hours and 12 hours) correspond to the circadian pattern. As a result, in addition to the circadian pattern, there is a shorter periodicity in the observed cortisol pattern [12]. Moreover, the 24-hour plasma cortisol profile consists of episodic release of 15 to 21 secretory events with varying magnitudes in a regular diurnal pattern, with the lowest amplitude occurring between 8pm and 2am, increasing rapidly throughout the late night, with the highest amplitude between 8am and 10am, and then, the amplitude declines throughout the day. The amount of cortisol released in each secretory episode is regulated by variations in amplitude rather than the frequency of secretory episodes [3].

Cortisol secretion is controlled by the hypothalamic pituitary adrenal axis (HPA), which is a self-regulated dynamic feedback neuroendocrine system [9]. In hypothalamus, SCN sends a harmonic circadian signal to the paraventricular nuclei (PVN), which leads to release of the CRH. CRH secreted into the hypophyseal portal blood

vessels induces release of ACTH from the anterior pituitary [3]. ACTH is synthesized and stored in the anterior pituitary gland. Synthesis and release can occur independently, and are stimulated by the neurohormone CRH [6]. Then, via stimulation of adrenal gland by ACTH, adrenal gland produces and secretes cortisol [13] [3]. After synthesis, cortisol diffuses into the circulation and is absorbed from the blood plasma by different tissues where it implements regulatory functions as a steroid hormone. Then, cortisol is cleared from the plasma by the liver [3]. Moreover, cortisol has a negative feedback effect on the hypothalamus and pituitary as well as CRH and ACTH secretion [9] [13] [3].

5.3 Mathematical Models for Cortisol Secretion

Different mathematical models of the HPA and cortisol secretion have been proposed in the literature. We will provide an overview of the proposed models. However, instead of using the notations used in each paper, the following notations will be used for all the models:

Glossary

C_r CRH

A ACTH

C_s Cortisol synthesized in the adrenal gland

C_a Cortisol concentration in the adrenal gland

C_p Cortisol concentration in the plasma space

R Glucocorticoid receptor

β_R Rate of infusion of CRH from the Hypothalamus

β_A Rate of infusion of ACTH from the anterior pituitary

β_I Rate of infusion of cortisol from the adrenal glands

β_{GR} Rate of degradation for glucocorticoid receptor

β_{PGR} Rate of production for glucocorticoid receptor

β_C Rate of clearance of cortisol from the plasma

β_P Rate of CRH production

β_D Rate of dissociation constant of cortisol receptor complex

K_1 Constant between zero and one

K_2 Inhibition Constant

K_3 Equilibrium binding affinity

S Circadian activator

F Stress to the HPA axis

5.3.1 Model I [3]

[3] introduces a stochastic differential equation model of diurnal cortisol patterns, assuming first-order kinetics for synthesis of cortisol in the adrenal gland, infusion of cortisol from adrenal gland to plasma, and clearance of cortisol from plasma by the liver (5.1-5.2), while making use of the timing of secretory events and circadian modulation of amplitude of secretory events:

$$\frac{dC_a}{dt} = -\beta_I C_a + C_s \ (Adrenal\ Gland) \tag{5.1}$$

$$\frac{dC_p}{dt} = \beta_I C_a - \beta_C C_p \ (Plasma) \tag{5.2}$$

where β_I and β_C are normal random variables with mean and variance obtained using cortisol data; C_s is a doubly stochastic pulsatile input which has a Gaussian circadian amplitude with a two-harmonic mean, and a mean-dependent variance, and a secretory event timing with gamma distributed interarrival times. Since no cortisol is stored in the adrenal gland, and cortisol synthesis is initiated by ACTH and is highly coupled to ACTH, it is possible to replace C_s with ACTH (variable A). In this model, Guassian noise is added to C_p to obtain the cortisol profile. The simulations obtained using this model have a plasma cortisol diurnal pattern, which agrees with

the physiology.

5.3.2 Model II [19]

[19] introduces five mathematical models of HPA axis based on a negative feedback mechanism with and without time delay, and shows that the systems introduced are stable and hence do not generate diurnal oscillations. They then introduce a sixth model, a circadian activator S with periodic stimulus from SCN (5.3-5.5), which results in a time-periodic pattern:

$$\frac{dC_r}{dt} = S\beta_P(1 - K_1\frac{C_a}{\beta_D + C_a}) - \beta_R C_r \ (Hypothalamus) \tag{5.3}$$

$$\frac{dA}{dt} = \beta_R C_r - \beta_A A \ (AnteriorPituitary) \tag{5.4}$$

$$\frac{dC_a}{dt} = \beta_A A - \beta_I C_a \ (AdrenalGland) \tag{5.5}$$

where S is either a value greater than one or one, and the CRH production rate β_P varies between zero and a positive value in a pulsatile manner.

This study suggests that HPA axis is asymptotically stable and does not oscillate at all; moreover, the time-periodic signal from SCN results in the observed cortisol concentration behavior. This model results in a smooth time-periodic pattern; however, it does not include any of the fluctuations observed in the actual cortisol profile, and even if some noise is added to the simulations obtained from this method, the resulting pattern still does not agree with the physiology because there are other trends in the data that can not be explained by adding noise (e.g. multiple local maximums). Moreover, parameters are chosen arbitrarily, and this model does not include all the external inputs to drive the system.

5.3.3 Model III [9]

[9] contains four differential equations. The first equation (equation 5.6) considers stress as the stimulus (the input to the system) that results in CRH release; also, cortisol inhibits the synthesis of CRH to regulate its own synthesis. Then, the second and third equations are coupled; one of the two equations (equation 5.7) shows that CRH results in ACTH release while glucocorticoid receptor (GR) and cortisol inhibit ACTH release; the other equation (equation 5.8) shows that GR and cortisol bind to each other with very fast kinetics. Finally, equation 5.9 shows that ACTH results in cortisol secretion.

$$\frac{dC_r}{dt} = \frac{1+F}{1+\frac{C_a}{K_1}} - \beta_R C_r \ (Hypothalamus) \tag{5.6}$$

$$\frac{dA}{dt} = \frac{C_r}{1+\frac{C_a R}{K_2}} - \beta_A A \ (AnteriorPituitary) \tag{5.7}$$

$$\frac{dR}{dt} = \frac{(C_a R)^2}{K_3 + (C_a R)^2} + \beta_{PGR} - \beta_{RG} R \ (AnteriorPituitary) \tag{5.8}$$

$$\frac{dC_a}{dt} = A - C_a \ (AdrenalGland) \tag{5.9}$$

The authors provide a plot that contains both the simulated cortisol data and the experimental cortisol data, which shows that the simulated results are very similar to the experimental data. They also provide a plot of the ACTH data, which is not released in bursts. [11] illustrates that ACTH should be secreted in bursts while [10] shows that ACTH does not have the same burst firings when stimulated by Metyrapone. Hence, we suspect that the model proposed by [9] is describing cortisol secretion under injection of some stimulus to account for stress. Also, the authors do not clarify whether they used a mathematical approach to find the stress as the input to the system or they were aware of the timing and magnitude of the stimulus injected to the subject, which resulted in the observed cortisol pattern.

5.3.4 Comparison of Models I-III

Comparing the discussed models, one can observe that equation 5.1 in model I, equation 5.5 in model II, and equation 5.9 in model III agree with each other with the only difference that the rate of cotisol synthesis in the adrenal glands and infusion of cortisol from the adrenal glands are different in these models. Considering that model I is the only model that uses actual data to estimate the rate, equation 5.1 (model I) is more reliable. Models II and III do not include a neural firing model or an euroendocrine model for CRH and ACTH while CRH and ACTH are released in pulsatile bursts.

In the literature, we found the following mathematical models for ACTH release via CRH regulation; [15] investigates CRH regulating ACTH secretion using the Hodgkin-Huxley(HH) mathematical model that results from the intracellular signaling system. In a later paper, [16] reduces the model in [15] to one with three differential equations. Later on, [20] includes a K^+ current which takes two values depending on the value of the action potential in the model in [15]. These models only include the ACTH release, and do not include a model for ACTH regulating cortisol release and cortisol secretion. Moreover, the neural firing model used in these papers is more complicated, and we suspect a simpler model (e.g. FHN with time varying spiking threshold) could be used for such modeling.

As discussed, reviewing the literature, we could not find a paper that provides a mathematical model for cortisol secretion that includes the entire process, starting from a deterministic neural firing model for secretion of CRH in the hypothalamus to cortisol secretion. In the next chapter, we will propose a more comprehensive model by bringing more pieces together and improving the current models. Considering that Model I describes the physiology and is capable of generating the fluctuations observed in the cortisol profile, we will use Model I as a starting point for this study.

Then, we will employ the FHN model with time-varying spiking threshold to study ACTH release. Our proposed model is different from model I in the sense that model I uses a doubly stochastic model for the input to the system while we will use a deterministic model, which includes a neural firing piece, and such model allows to study the kind of pulsatile mechanism the body uses for hormone secretion. Also, we include the negative feedback effect of cortisol in our model. Moreover, our proposed ACTH secretion model is simpler than the existing dynamical models for ACTH secretion.

Chapter 6

A Feedback Control Model of Cortisol Secretion using FHN Model with Time-varying Spiking Threshold

6.1 Model I: A Linear Model for Cortisol Secretion

As discussed in the previous chapter, reviewing the literature, we could not find a paper that provides a mathematical model for cortisol secretion that includes the entire process, starting from a deterministic neural firing model for secretion of CRH in the hypothalamus to cortisol secretion. Considering that Model I [3] describes the physiology and is capable of generating the fluctuations observed in the cortisol profile, we will use Model I as a starting point for this study:

$$\frac{dC_a}{dt} = -\beta_I C_a + C_s \ (Adrenal\ Gland) \tag{6.1}$$

$$\frac{dC_p}{dt} = \beta_I C_a - \beta_C C_p \ (Plasma) \tag{6.2}$$

The variables and the parameters of this model were introduced in the previous chapter. Model I [3] estimates β_I and β_C to be normal random variables with mean values 2.71 and 0.646, respectively. Throughout this chapter, we will assume that these mean values are the parameter values in the described model.

6.2 Obtaining the Input to Model I

The solutions to the linear time-invariant state equations in model I are as follows:

$$C_a(t) = e^{-\beta_I t} C_a(0) + \int_0^t e^{-\beta_I (t-\tau)} C_s d\tau \ (Adrenal\ Gland) \tag{6.3}$$

$$C_p(t) = e^{-\beta_C t} C_p(0) + \int_0^t e^{-\beta_C (t-\tau)} \beta_I C_a d\tau \ (Plasma) \tag{6.4}$$

When the cortisol level in blood is available, one could rewrite the above system by replacing the two integrals by two convolutions. Then, considering that the datasets are discrete, one could rewrite each convolution in the form of a Toeplitz matrix. Let G_a be the Toeplitz matrix that corresponds to the convolution in 6.3 and let G_p be the Toeplitz matrix that corresponds to the convolution in 6.4. In other words, when cortisol data is available at times t_0, t_1, ...,t_n, one could rewrite the convolutions in equations 6.3 and 6.4 as:

$$\begin{pmatrix} e^{-\beta_I t_0} & 0 & 0 & \cdots & 0 \\ e^{-\beta_I t_1} & e^{-\beta_I t_0} & 0 & \cdots & 0 \\ \vdots & \vdots & \vdots & \ddots & \vdots \\ e^{-\beta_I t_n} & e^{-\beta_I t_{n-1}} & e^{-\beta_I t_{n-2}} & \cdots & e^{-\beta_I t_0} \end{pmatrix} \begin{pmatrix} C_s(t_0) \\ C_s(t_1) \\ \vdots \\ C_s(t_n) \end{pmatrix} = G_a C_s$$

$$\begin{pmatrix} \beta_I e^{-\beta_C t_0} & 0 & 0 & \cdots & 0 \\ \beta_I e^{-\beta_C t_1} & \beta_I e^{-\beta_C t_0} & 0 & \cdots & 0 \\ \vdots & \vdots & \vdots & \ddots & \vdots \\ \beta_I e^{-\beta_C t_n} & \beta_I e^{-\beta_C t_{n-1}} & \beta_I e^{-\beta_C t_{n-2}} & \cdots & \beta_I e^{-\beta_C t_0} \end{pmatrix} \begin{pmatrix} C_a(t_0) \\ C_a(t_1) \\ \vdots \\ C_a(t_n) \end{pmatrix} = G_p C_a$$

Then, let u_p=$e^{-\beta_C t} C_p(t_0)$ and u_a=$e^{-\beta_I t} C_a(t_0)$. When one has access to the cortisol data, $C_p(t_0)$ is available, and hence, u_p is a known quantity. Then, by formulating the optimization problem 6.5, one could solve for C_a; hence, $C_a(t_0)$ and u_a will be known quantities. In order to obtain C_s, one could solve the optimization problem 6.6:

$$min_{C_a>0} \|C_p - u_p - G_p C_a\|^2 \tag{6.5}$$

$$min_{C_s>0} \|C_a - u_a - G_a C_s\|^2 \tag{6.6}$$

The value of C_s obtained using this formulation is an estimate of the pulsatile input to the system in model I.

6.3 Modeling the pulsatile Input that Induces C_s Secretion

As mentioned in the previous chapter, C_s secretion is highly coupled to ACTH secretion, and ACTH is induced by CRH. Considering that CRH has a varying frequency secretion profile, one could model the CRH secretion using the varying frequency neural firing model described in chapter 2 where a two-harmonic spiking threshold was used in the FHN model. Considering that the circadian rhythm plays an important role in the cortisol secretion, periods T=24, and T=12 could be used as the periods of such a two-harmonic function. Let v_{in} be the output of the FHN model with a two-harmonic spiking threshold. Then, let the CRH secreted be C_r=max(2.5v_{in},0). C_r induces the ACTH secretion; however, the ACTH secreted is affected by the neg-

ative feedback effect of the cortisol level. In the following section, we will describe how one could model this negative effect.

6.4 Negative Feedback Effect of Cortisol Level

Our goal is to model C_s in a deterministic manner by using a neural spiking model as well as feedback control. We suspect that the negative feedback effect of the cortisol level in plasma on ACTH secretion and cortisol secretion can be modeled as a tracking problem. In other words, if the cortisol level is below a certain time-varying threshold, there will be ACTH secretion, and if the cortisol level is above a certain threshold, the negative feedback effect of the cortisol level prevents any ACTH secretion and hence no more cortisol will be secreted.

In order to obtain such a time-varying threshold, one could first inspect the C_s time-series plot to obtain the times at which there is a pulsatile secretion. Then, form a dataset that includes the plasma cortisol levels corresponding to the time at which there is a pulsatile secretion in C_s. Then, using multiple regression, one could fit this new dataset to a three-harmonic function of the form:

$y_{thresh} = \alpha + \beta cos(\frac{2\pi t}{24}) + \gamma sin(\frac{2\pi t}{24}) + \zeta cos(\frac{2\pi t}{12}) + \kappa sin(\frac{2\pi t}{12}) + \varsigma cos(\frac{2\pi t}{2}) + \varrho sin(\frac{2\pi t}{2})$

Periods 24, 12, and 2 are chosen because as mentioned in the previous chapter the ultradian analysis of cortisol shows significant periods of 24 hours, 12 hours, and 2 hours [12]. The ACTH profile (A) is induced by the secreted CRH and is suppressed by the cortisol level. Hence, one could model the ACTH profile as:

$$A(t) = \begin{cases} C_r(t) & y_{thresh} > C_p \\ 0 & y_{thresh} < C_p \end{cases}$$

Moreover, $C_s(t)$=kA(t), where k is a constant gain.

Fig. 6-1 is a block diagram of the described model. We simulated the 24-hour cortisol profile using the following parameters and functions:

In the FHN part of the model, a=100, I=1, and c=0.28 were used, and b was defined as:

$$b = \frac{10 - 6cos(\frac{2\pi}{24}(t+9)) + 3.5sin(\frac{2\pi}{24}(t+9)) - 3.5cos(\frac{2\pi}{12}(t+9)) - 1.1720sin(\frac{2\pi}{12}(t+9))}{25}$$

$$y_{thresh} = -5.8071cos(\frac{2\pi t}{24}) - 1.1020sin(\frac{2\pi t}{24}) - 0.9184cos(\frac{2\pi t}{12}) - 2.8927sin(\frac{2\pi t}{12}) + 0.1259cos(\frac{2\pi t}{2}) + 0.6564sin(\frac{2\pi t}{2}) + 6.5595$$

Moreover, k=100 was used.

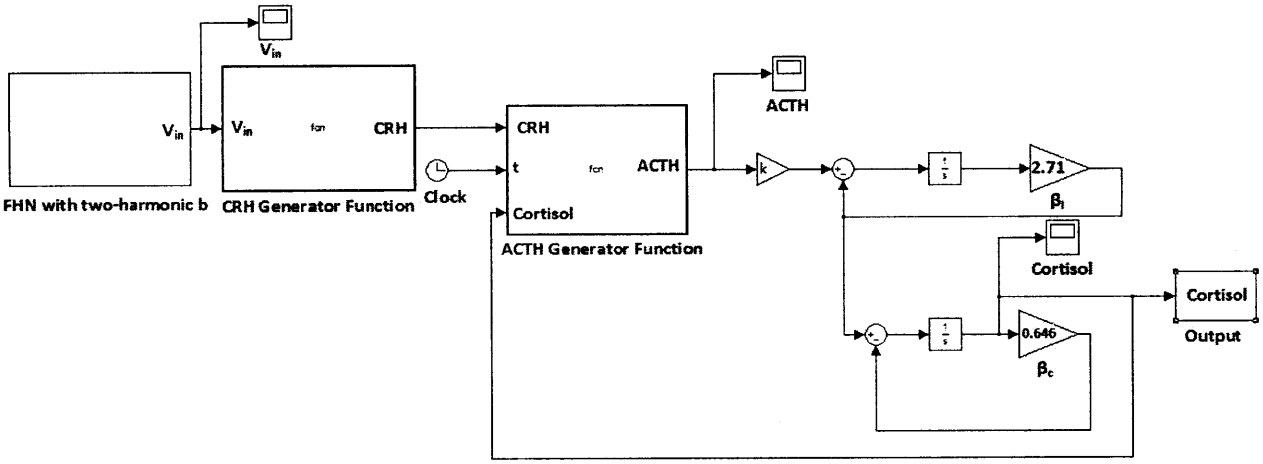

Figure 6-1: Simulink Block Diagram of the Cortisol Feedback Control Model

Fig. 6-2 is the 24-hour cortisol profile obtained using this simulation. This profile closely resembles the profile that cortisol follows, i.e. cortisol level is at the highest amplitude between 8am and 10am, and declines throughout the day; then, increases rapidly through the late night (see Fig. 8 in [3]).

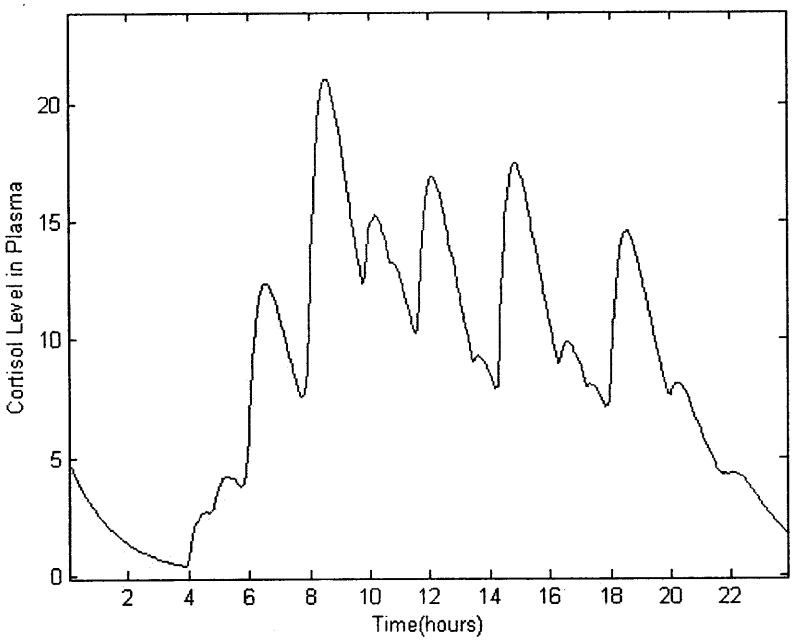

Figure 6-2: Simulated 24-hour Cortisol Profile in Plasma

Chapter 7

Conclusion and Future Work

7.1 Conclusion

The proposed approach in extending the FHN model by varying the parameters of FHN allows for simulating more complex behaviors than the ones that were possible by keeping the parameters constant. In this thesis, variations in the threshold between electrical silence and electrical firing were investigated. Then, an estimation algorithm that exploits the fast-slow dynamics of FHN was proposed.

For constant b, the proposed parameter estimation algorithm performed better than the EKF when the sampling rate was not very high or when the sensor noise covariance was not very low. For time-varying b, this parameter estimation method performed better than EKF when the sampling rate was low. Another advantage of this estimation method over EKF is that for cases that the structure of b is unknown e.g. the underlying structure of b that governs the release of the cortopin releasing hormone, discrete b estimates can be obtained using our method to add insight to the underlying structure. On the other hand, EKF can not estimate the coefficients if the underlying structure of b is not known.

One application of FHN model with time-varying threshold is modeling the secretion process for some of the hormones such as cortisol or growth hormone. In this thesis,

FHN model with time-varying spiking threshold was used for modeling the cortisol secretion. Moreover, a more comprehensive model for cortisol secretion was provided by extending the model in [3] and including the negative feedback effect of cortisol, and looking at the cortisol secretion as a tracking problem.

7.2 Future Work

In our future work, we will extend our model and estimation method to other parameters of the FHN model. We also plan to explore the physiological factors determining the parameter variations that lead to variations in neural firing patterns.
Moreover, we will obtain cortisol data to implement our feedback control model on cortisol data, and analytically investigate trackability in the cortisol secretion process. We might also add to the current feedback control model of cortisol another piece that includes the negative feedback effect of cortisol on CRH secretion. We could also use a similar approach to study growth hormone, luteinizing hormone, follicle-stimulating hormone, or thyroid hormone. We also plan to study why the body uses a pulsatile mechanism for hormone secretion, and why such a mechanism is efficient in conserving energy in the body. Furthermore, we plan to study a network of neurons that are coupled to each other, and result in neural spiking with varying amplitude as a result of their synchronization.

Bibliography

[1] Brown D, Herbison A.E., Robinson J.E., Marrs R.W., Leng G. "Modeling the luteinizing hormone-releasing hormone pulse generator." *Journal of Neuroenocrinology*, Vol. 63(3):869-879,1994.

[2] Brown E.N., Choe Y, Luithardt H, Czeisler C.A. "A statistical model of human core-temperature circadian rhythm." *American Journal of Physiology Endocrinology and Metabolism*, Vol. 279:E669E683, 2000.

[3] Brown E.N., Meehan P.M., Dempster A.P. "A stochastic differential equation model of diurnal cortisol patterns." *American Journal of Physiology Endocrinology and Metabolism*, Vol. 280:E450E461, 2001.

[4] Buhry L, Saighi A, Giremus E, Renaud S, "Parameter estimation of the Hodgkin-Huxley model using metaheuristics: applications to neuromimetic analog integrated circuits." *IEEE Biomedical Circuits and Systems*, 173176, 2008.

[5] Churilov A, Medvedev A, Shepeljavyi A. "Mathematical model of non-basal testosterone regulation in the male by pulse modulated feedback." *Automatica* Vol.45:78-85, 2009.

[6] Dallman M.F. and E.F. Yates. "Dynamic Asymmetries in the Corticosteroid Feedback Path and Distribution-Metabolism-Binding Elements of the Adrenocortical System." *Ann. NY Acad. Sci.*, vol. 156: 696-721, 1969.

[7] Izhikevich E.M. "Which Model to Use for Cortical Spiking Neurons?" *IEEE Trans. on Neural Networks (Special Issue on Temporal Coding)*, 2004.

[8] Izhikevich E.M., Dynamical Systems in Neuroscience: The Geometry of Excitability and Bursting, MIT Press, 2007.

[9] Gupta Sh, Aslakson E, Gurbaxani B.M., Vernon S.D. "Inclusion of the glucocorticoid receptor in a hypothalamic pituitary adrenal axis model reveals bistability." *Theoretical Biology and Medical Modelling*, 4:8, 2007.

[10] Keenan D.M. and J.D. Veldhuis. "Cortisol feedback state governs adrenocorticotropin secretory-burst shape, frequency, and mass in a dual-waveform construct: time of day-dependent regulation." *AM J Physiol Regulatory Integrative Comp Physiol*, Vol. 285: 950-961, 2003.

[11] Keenan D.M., Roelfsema F, Veldhuis J.D. "Endogenous ACTH concentration-dependent drive of pulsatile cortisol secretion in the human." *Am J Physiol Endocrinal Metab*, Vol. 287:652-661, 2004.

[12] Korszun A, Young E.A., Singer K, Carlson N.E., Brown M.B., Crofford L. "Basal Circadian Cortisol Secretion in Women with Temporomandibular Disorders." *Journal of Dental Research*, Vol. 81: 279-283, 2002.

[13] Kyrylov V, Severyanova L.A., Vieira A."Modeling Robust Oscillatory Behavior of the Hypothalamic-Pituitary-Adrenal Axis." *IEEE Transaction on Biomedical Engineering*, Vol. 52, No. 12:1977-1983, 2005.

[14] Labbi A, Milanese R, Bosch H, "Gray-Level Object Segmentation with a Network of FitzHugh-Nagumo Oscillators." *Biological and Artificial Computation: from Neuroscience to Technology: Proceedings*, Vol. 1240. Berlin [etc.]: Springer, 1997. 1075-084.

[15] LeBeau A.P., Robson A.B., McKinnon A.E., Donald R.A., Sneyd J. "Generation of Action Potentials in a Mathematical Model of Corticotrophs." *Biophysical Journal*, Vol. 73: 1263-1275, 1997.

[16] LeBeau A.P., Robson A.B., McKinnon A.E., Sneyd J."Analysis of a Reduced Model of Corticotrophs Action Potentials." *J. Theor. Biol.*, Vol. 192: 319-339, 1998.

[17] Leng G and D Brown. "The Origins and Significance of Pulsatility in Hormone Secretion from the Pituitary." *Journal of Neuroenocrinology*, Vol. 9:493-513,1997.

[18] Rinzel J, Keener J.P., "Hopf Bifurcation to Repetitive Activity in Nerve." *SIAM Journal on Applied Mathematics*, Vol. 43(4): 907-922, 1983.

[19] Savic D and S Jelic. "A mathematical model of the hypothalamo-pituitary-adrenocortical system and its stability analysis." *Chaos Solutions and Fractals*, Vol. 26:427-436, 2005.

[20] Shorten P.R., Robson A.B., McKinnon AE, Wall DJN, "CRH-induced Electrical Activity and Calcium Signaling in Pituitary Corticotrophs." *J. Theor. Biol.*, Vol. 206: 395-405, 2000.

[21] Terasawa E. "Luteinizing hormone-releasing hormone (LHRH) neurons: mechanism of pulsatile LHRH release." *Vitamins and Hormones*, Vol. 63: 91-129, 2001.

[22] Tokuda I, Parlitz U, Illing L, Kennel M, Abarbanel H. "Parameter Estimation for Neuron Models." San Diego: 2002.

[23] Tsuji Sh, Ueta T, Kawakami H, Aihara K. "A Advanced Design Method of Bursting In FitzHugh-Nagumo Model." *IEEE International Symposium on Circuits and Systems*, Vol. 1:I-389-I392, 2002.

[24] Tuckwel H.C.l, Rodriguez R, Wan F.Y.M., "Determination of Firing Times for the Stochastic Fitzhugh-Nagumo Neuronal Model." *Neural Computation*, Vol. 15(1):143-159, 2003.